Remote sensing image fusion method based on the contourlet coefficients' correlativity of directional region

WANG Xianghai[1,2], WEI Tingting[2], ZHOU Zhiguang[3]

1. *Liaoning Key Laboratory of Physical Geography and Geomatics, Liaoning Normal University, Liaoning Dalian* 116029, *China*;
2. *College of Computer and Information Technology, Liaoning Normal University, Liaoning Dalian* 116029, *China*;
3. *State Key of CAD&CG, Zhejiang University, Zhejiang Hangzhou* 310027, *China*

Abstract: In this paper, we analyze the directional characteristics of contourlet coefficients in high frequency subbands of remote sensing images. And then we find that each coefficient in these subbands has obvious directionality. Based on this directional characteristic, this paper proposes a novel image fusion algorithm for remote sensing images. First, we separately perform contourlet transform on the intensity component of the multi-spectral remote sensing image obtained by IHS transform, and the panchromatic remote sensing image. Second, we choose the low frequency coefficients of multi-spectral image's intensity component to form the low frequency subband of target image. Subsequently, we compare the directional matching degree of the high frequency coefficients of the panchromatic image with those of the multi-spectral image's intensity component to determine the high frequency subbands of target image. Finally, the target image is obtained by inverse contourlet transform and inverse IHS transform. Extensive experimental results show that the proposed method is superior to conventional methods in terms of entropy, joint entropy, and average gradient. It can enhance the spatial resolution of target images. Meanwhile, it well preserves the color information of multi-spectral images.

Key words: remote sensing image fusion, contourlet transform, correlativity of directional region, fusion operator

CLC number: TP751.1 **Document code:** A

Citation format: Wang X H, Wei T T, Zhou Z G. 2010. Remote sensing image fusion method based on the contourlet coefficients' correlativity of directional region. *Journal of Remote Sensing*. **14**(5): 905—916

1 INTRODUCTION

In recent years, as an important branch of remote sensing image processing technology, remote sensing image fusion technologies have been widely applied, especially in the field of resource exploration, environmental monitoring, region analysis, project plan, global macro study and so on(Li *et al*., 2004; Lin *et al*., 2009; Li *et al*., 2008). Through combining the merit of low-resolution multi-spectral images and high-resolution panchromatic images, the technologies can make the target images higher color resolution and higher spatial resolution at the same time, so we can obtain timely and reliable remote sensing information. Further, it can enhance the availability of data (Zhang *et al*., 2005; Chen *et al*., 2005). The three most popular fusion methods are based on IHS, wavelet and contourlet transform. The first one replaces the Intensity component (I) of multi-spectral image with panchromatic image (Tu *et al*., 2004; Choi, 2006). It enhances the fused image's spatial information but distorts the color information. On the basis of IHS transform, to some extent, the second one makes use of multi-scale characteristics of the wavelet transform to obtain a more abundant high frequency information (Wu *et al*., 2006; Liu *et al*., 2004). The wavelet transform has the best approximation in the point singularity of the signal, but its capability of sparse representation is relatively limited for two-dimensional images or higher dimensional data. As the supported interval of the two-dimensional separable wavelet's basis functions is a square, it is isotropic and can denote only two-dimensional or high-dimensional signal's linear singularity in the directions of vertical, horizontal and diagonal. Most of the objects' edges are smooth in remote sensing image, but this allows natural images' singular points not independent but aggregated into some singular curve with a certain geometrical features. In this case, along the singularity of the curve on the edge direction, the wavelet transform can not use the data itself effectively to capture the unique geometrical features of the image because of its isotropic basis functions, so it can not provide the representation of the image with the best and the sparse form. In the past few years, as a result of their excellent anisotropic characteristic, "multi-scale geometric analysis (MGA)" (Jiao & Tan, 2003), which developed from the wavelet theory, became a better method to process two or higher dimensional data. It has solved

Received: 2009-10-16; **Accepted**: 2010-01-15

Foundation: Natural Foundation of Liaoning (No. 20072156), Liaoning BaiQianWan Talents Program (No. 2008921036) and Jiangsu Key Laboratory's Open-end Foundation of Image Processing and Image Communication of Nanjing University of Posts & Telecommunications (No. ZK207008).

Author biography: WANG Xianghai (1965—), male, Professor of Liaoning Normal University and Senior Member of the CCF, mainly interests in multimedia information processing and computer graphics. E-mail: xhwang@lnnu.edu.cn.

the problem that the wavelet can not effectively represent the singularity of the edge and outline of high-dimensional data. As one key member of the MGA, contourlet transform (Do & Vetterli, 2005) is considerably concerned in the field of remote sensing image fusion (Zheng *et al*., 2006; Chen *et al*., 2006; Zhang & Guo, 2008; Liu *et al*., 2008). It has dramatically improved the inaccuracy conditions of fused edge and texture information based on the wavelet transform. Therefore the study for the field is still on the initial stage, a lot of problems need to be studied further, and the fused image's quality needs to be improved, too.

After analyzing and collecting the directional characteristics of contourlet coefficients in high frequency subbands of remote sensing images, in this paper, we find that high frequency coefficients of remote sensing images have strong correlativity of directional region. So, on this basis, we propose a novel image fusion method of remote sensing images based on contourlet coefficients' correlativity of directional region. Besides improving fused image's spatial resolution, our method can better preserve original multi-spectral image's color information. Experiment results show that our method can make the target image clearer, and objective evaluative criteria better in entropy, clarity, bias index, etc.

2 THE ANALYSIS OF DIRECTIONAL CHARACTERISTIC OF CONTOURLET COEFFICIENTS IN HIGH FREQUENCY SUBBANDS

Do and Vetterli (2005) proposed a Pyramidal Directional Filter Band (PDFB), namely contourlet transform. Firstly, the Laplacian pyramid (LP) transform is used to do multi-scale decomposition, namely the images are decomposed into different resolution levels with different sizes, which can capture two-dimensional images' singular points. Through the LP transform, the original signal is decomposed into a low frequency signal and D-value's bandpass signal between the original signal and prediction signal; Secondly, the Directional Filter Bank (DFB) is used to filter the bandpass signal from each LP channel, which synthesizes the same directional singular points into a coefficient. As having a variational "long strip" structure in length-width ratio, it can effectively capture images' line singularity and surface singularity. Consequently, contourlet transform gets not only better non-linear approximation, but also better multi-resolution, local orientation, multi-directional, neighbor sampling and anisotropic. It can represent the image more sparsely compared with the wavelet transform (Asmare *et al*., 2009; Xiaobo *et al*., 2007). The processing diagram of image's PDFB decomposition is shown in Fig.1. The contourlet decomposition of the remote sensing image is shown in Fig. 2.

The traditional image fusion methods mostly take the correlativity of the eight neighborhood coefficients as the judgment evidence for image fusion (Di *et al*., 2006). However, we find that the distribution of contourlet high frequency coefficients

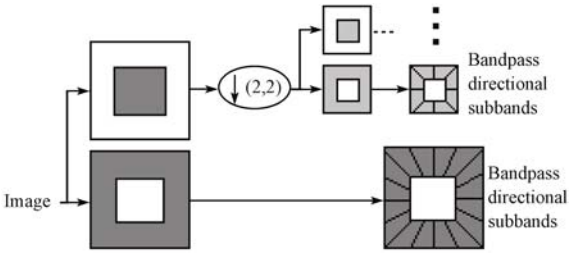

Fig. 1 Processing diagram of image's PDFB decomposition

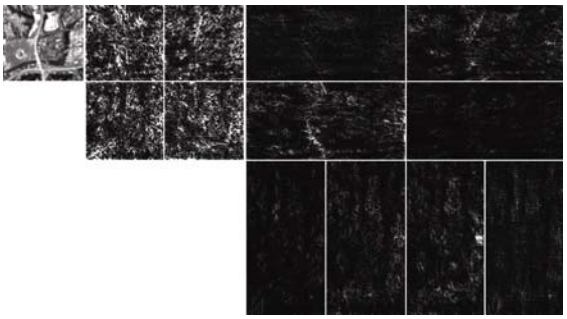

Fig. 2 Contourlet decomposition of the remote sensing image

has a certain directional characteristic. Here, panchromatic image pan and multi-spectral image ms are used to be source images, which are in 256×256 size. We use the template of directional region as shown in Fig. 3 to collect the high frequency coefficients, and take the variance as the judgment criteria. If the variance of directional region is less than variance of eight neighborhood, it indicates that the directional characteristic is stronger. If the variance of directional region is more than the variance of eight-neighborhood, it indicates that the correlativity of eight-neighborhood is stronger. The four templates and eight templates in Fig. 3(a), Fig. 3(b) respectively correspond to 4 subbands of the 2nd level and 8 subbands of the 3rd level in different directions of contourlet transform.

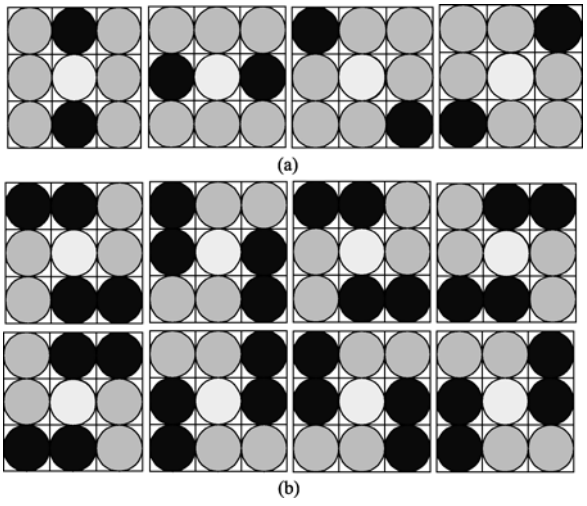

Fig. 3 Template of directional region in the high frequency subbands' coefficents of remote sensing image
(a) Four templates corresponding to 4 subbands of the 2nd level;
(b) Eight templates corresponding to 8 subbands of the 3rd level

The high frequency coefficients' correlativity of directional region is shown in Table 1. The subbands of NO.1—NO.4 and NO.5—NO.12, respectively represent the correlativity's statistics of directional region of four subbands of 2nd level and 8 subbands of the 3rd level, namely, by comparing the variance of directional region and eight-neighborhood coefficients, they are the proportions of satisfying correlativity's coefficients of directional region accounted for the sum of subbands' coefficients. The Table 1 shows that the coefficients' proportions satisfying the correlativity of directional region are all over 50%. It indicates the directional characteristic of contourlet coefficients in high frequency subbands is stronger than the correlativity of eight-neighborhood.

Table 1 PAN and MS correlativity's statistics of directional region

Subband	PAN/%	MS-*R*/%	MS-*G*/%	MS-*B*/%
1	82.23	91.02	89.85	90.45
2	62.59	59.60	60.04	59.68
3	75.91	72.71	72.87	73.83
4	81.63	90.63	90.45	90.11
5	59.86	58.15	58.61	58.60
6	58.46	60.59	60.33	60.59
7	55.54	54.26	53.60	54.34
8	55.93	55.94	55.34	55.90
9	57.57	58.35	58.36	58.53
10	56.89	60.23	60.91	61.19
11	58.56	59.87	60.36	60.20
12	56.93	56.69	57.23	57.28

3 REMOTE SENSING IMAGE FUSION METHOD BASED ON THE CONTOURLET COEFFICIENTS' CORRELATIVITY OF DIRECTIONAL REGION

3.1 Basic process of our method

From the analytical and statistical results in part 2, we can know that there is a certain directional characteristic of contourlet coefficients in high frequency subbands, which allows the current fused coefficients and its eight-neighborhood coefficients of the high-frequency subbands to exist differences in "close" level. So, by using the coefficients closely concerned with the fused coefficients, you will improve the quality of the target image.

Different from the coefficients displacement method of traditional contourlet transform, in this paper, according to the high frequency subbands' correlativity of directional region, we determine the fused image's Intensity component (*I*) in high frequency coefficients by comparing with to be fused coefficients' matching degree of directional region. Fig.4 is the framework of the proposed method.

The fused rule of our method is as follows:

Step1 Perform IHS transform on the multi-spectral image;

Step2 The IHS transformed multi-spectral image's Intensity component (*I*) and the panchromatic image are respectively contourlet transformed;

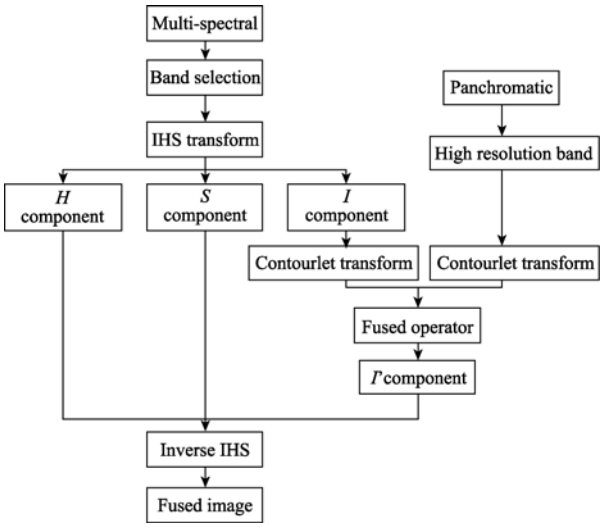

Fig. 4 Schematic diagram for image fusion using this method

Step3 The low frequency information of fused image's Intensity component (*I*) is the low frequency information of multi-spectral image's Intensity component (*I*);

Step4 Calculate and compare with the matching degree of directional region between the high frequency coefficients of panchromatic image and multi-spectral image's Intensity component (*I*), we can gain the high frequency coefficients of fused image's Intensity component (*I*);

Step5 The fused image's IHS transformed result is the resultant image by inverse contourlet transform;

Step6 The target image can be obtained by inverse IHS transform.

3.2 Selection of fused operator

The multi-spectral image is strong-spectral and provides significant background information. By using contourlet coefficients of multi-spectral image's Intensity component (*I*) of IHS transform and panchromatic image, the low frequency information of fused image's Intensity component (*I*) is the low frequency information of multi-spectral image's Intensity component (*I*) and further guarantee fused image's multi-spectral characteristic; For the fused process of high frequency coefficients, we propose the fused operator of contourlet coefficients' correlativity of directional region by adopting the template of directional region in the 2nd chapter, specific steps are as follows:

Step1 Calculate high frequency coefficients' energy of directional region of the corresponding position using Eq. (1), where α indicates the directional template which aims at different subbands (see Fig. 3), $f_k(i, j)$ and $E_k(i, j)$, k=1,2, are the fusion coefficient of directional region and the region energy of the corresponding coefficient of directional template, respectively, of the first k images.

$$E_k(i,j) = \sum_{f_k(i,j)\in\alpha} (f_k(i,j))^2 \tag{1}$$

Step2 Calculate the matching degree of directional region

through Eq. (2), where $M(x, y)$ is the matching degree of directional region of corresponding high frequency coefficients.

$$M(i,j)=\frac{2\sum_{f_k(i,j)\in\alpha}(f_1(i,j)\cdot f_2(i,j))}{E_1(i,j)+E_2(i,j)} \quad (2)$$

Step3 Compare the matching degree of directional region with the threshold value β (β can be obtained through the test statistics and is selected as 0.9 in the following test), and further determine the high frequency coefficients of fused image, specific operations are as follows:

If $M(x,y)<\beta$

$$f(x,y)=\begin{cases} f_1(x,y) & \text{if} \quad E_1>E_2 \\ f_2(x,y) & \text{others} \end{cases}$$

If $M(x,y)\geqslant\beta$, then

$$f(x,y)=\begin{cases} w_{\max} f_1(x,y)+ w_{\min} f_2(x,y) & \text{if} \quad E_1>E_2 \\ w_{\min} f_1(x,y)+ w_{\max} f_2(x,y) & \text{others} \end{cases}$$

where $w_{\min}=\frac{1-M(x,y)}{2(1-\beta)}$ and $w_{\max}$=1−$w_{\min}$ are respectively weighting coefficients of to be fused coefficients, $f(x,y)$ is the final fused coefficients.

Step4 In terms of the above mentioned steps, traverse all the high frequency coefficient points in different directions, and ultimately, gain the high frequency coefficients of fused image's I.

4 EXPERIMENTS AND ANALYSIS

We use three sets of standard remote sensing images to test this method: The first group images are the 80-meter resolution multi-spectral image ms and the 32 meters resolution panchromatic image pan. The second group images are tms image and spots image taken from ERDAS examples library. The third group images are multi-spectral image tm taken from the United States landsat5 and panchromatic image spot taken from the French satellite. We compare our scheme with the remote sensing fusion method based on the traditional IHS, wavelet and contourlet transform. Fig.5—7 are the corresponding ones to three sets of images' fused results respectively.

Fig.5—Fig.7 show that the obtained fused images by our method include more of texture and color information than its counterparts. In this way we can preserve spectral characteristic better.

In addition, we use four objective indicators to compare the experimental results of image fusion. These four objective indicators are entropy, joint entropy, average gradient and bias index. Objective evaluation for fusing remote sensing image is shown in Table 2.

In Table 2, we can see that the fused image which is used our method is the best in entropy, joint entropy, average gradient and bias index. The details: (1) Besides improving fused image's spatial resolution of the ms image and pan image, our method can better retain the original multi-spectral image's color information. (2) Fusing the tms image and spots image, the entropy, the joint entropy and average gradient are the biggest, the bias index is the smallest, so our method has better preserved images' spatial resolution and color resolution. (3) Fusing tm image and spot image, our entropy and joint entropy are smaller than the IHS transform, but the average gradient value is the biggest and the bias index is the smallest. This shows that the IHS transform is at the expense of spectral information for the spatial information, and the image is slightly clearer, but the color distortion is more serious. However, besides improving fused image's spatial resolution, our method can better retain the original multi-spectral image's color information.

Though the contourlet transform is evident in anisotropy relative to the wavelet transform and is a greater advantage in the edge contour extraction, due to two low-pass filters of LP transform in contourlet, which does not meet the Nyquist sampling law, results in stop-band cutoff frequency greater than $\pi/2$, leads to contourlet transform spectrum aliasing (Feng *et al*., 2008), generates Pseudo-Gibbs phenomenon and further impacts the results of the image fusion. In recent years, there have been some anti-aliasing contourlet transform, as the typical example is the nonsubsampled contourlet transform (Cunha *et al*., 2006), which is shift-invariant and has overcome the frequency

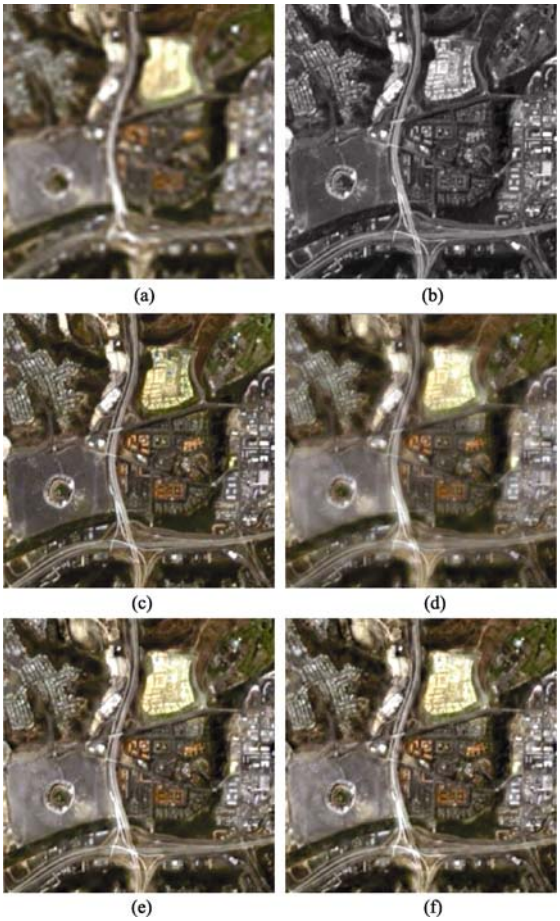

Fig. 5 The "MS" and "PAN" source images and fusion results
(a) Source image MS; (b) Source image PAN; (c) IHS method; (d) Wavelet+IHS method; (e) Contourlet replacement method; (f) This method

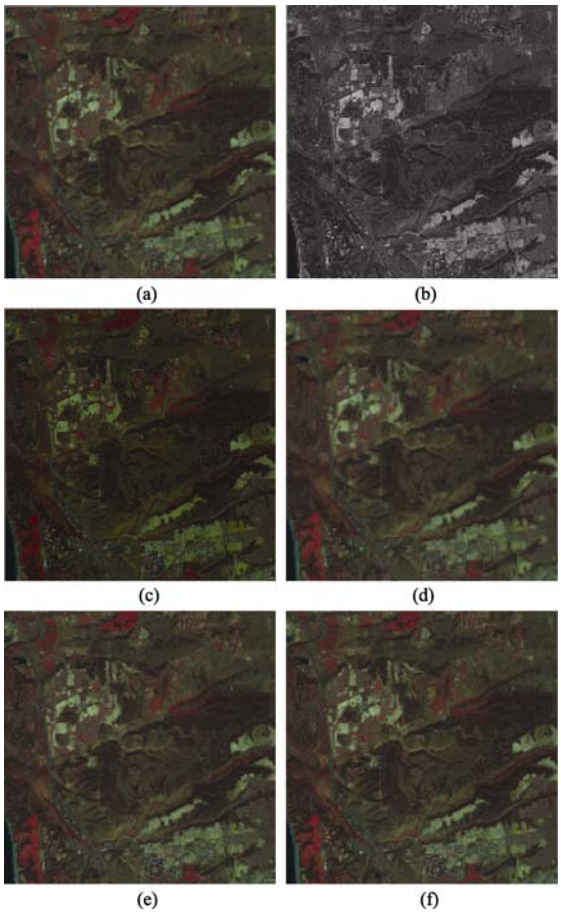

Fig. 6 The "Tm" and "SPOT" source images and fusion results
(a) Source image Tm; (b) Source image SPOT; (c) IHS method; (d) Wavelet+IHS method; (e) Contourlet replacement method; (f) This method

aliasing effect. Through extensive experiments, we find that orientation characteristic of the transformed subbands coefficients is weakened, but space and time complexity are increased. It has affect real-time processing of the image fusion. After weighing the fused efficiency and fused effect, we use the stronger coefficients' correlativity of directional region in high-frequency subband and further ascertain the corresponding fused operator, which highlights and emphasizes directional characteristic of each subband coefficients. From the experiment results, we can see our method can improve frequency aliasing effect comparing with the traditional contourlet replacement method.

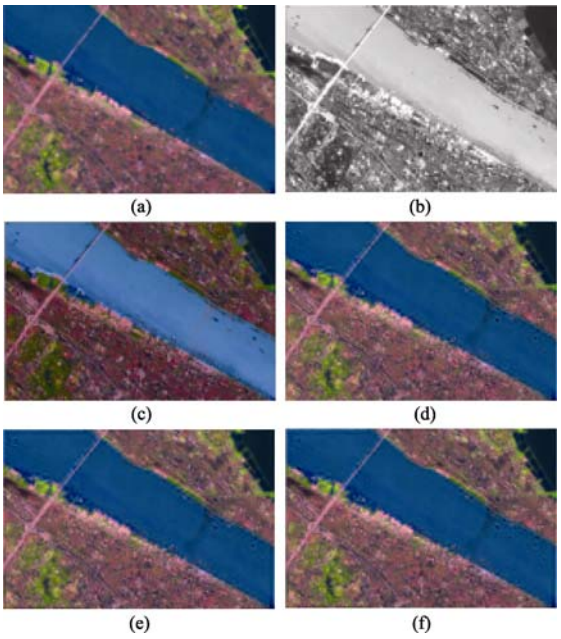

Fig. 7 The "TM" and "SPOT" source images and fusion results
(a) Source image TM; (b) Source image SPOT; (c) IHS method; (d) Wavelet+IHS method; (e) Contourlet replacement method; (f) This method

Table 2 Objective performance corresponding to the four methods

Evaluation \ Method			IHS	Wavelet+IHS	Contourlet replacement	Our method
Entropy	The first group	*R*	6.7339	7.5222	7.5201	7.5417
		G	6.6053	7.4974	7.4938	7.5159
		B	6.2987	7.4875	7.4868	7.5057
	The second group	*R*	5.9393	6.2173	6.2178	6.2197
		G	6.2169	6.3742	6.3741	6.3789
		B	5.6608	5.7921	5.7927	5.7909
	The third group	*R*	6.9112	7.0800	7.1189	7.1225
		G	6.6743	6.3017	6.3372	6.3381
		B	7.0773	6.5630	6.6185	6.6074
Joint entropy	The first group		19.6379	22.5071	22.5007	22.5646
	The second group		17.8170	18.3837	18.3846	18.3895
	The third group		20.6628	19.9447	20.0745	20.0680
Average gradient	The first group	*R*	4.0386	4.4337	4.4320	4.7659
		G	3.9484	4.3637	4.3552	4.6900
		B	3.8127	4.3660	4.3600	4.6814
	The second group	*R*	3.3845	3.4358	3.4325	3.4463
		G	3.3906	3.4407	3.4372	3.4563
		B	3.3160	3.3516	3.3477	3.3530
	The third group	*R*	3.7002	3.7966	3.7847	3.8747
		G	3.3228	3.4175	3.4064	3.4751
		B	3.4723	3.4672	3.4561	3.4846
Bias index	The first group		0.0285	0.0929	0.1098	0.0651
	The second group		0.0051	0.0176	0.0179	0.0164
	The third group		0.3847	0.0146	0.0219	0.0129

5 CONCLUSION

In this paper, we have firstly analyzed directional correlativity of the contourlet coefficients in high frequency subbands of remote sensing images. Then we find that the coefficients in each high frequency subbands have a certain correlativity of directional region. The statistical results have verified the given conclusion, and meanwhile, we have given the template of directional region in each high frequency subbands. On this basis, we propose a novel remote sensing image fusion method based on the contourlet coefficients' correlativity of directional region. Firstly, the Intensity component (*I*) of the multi-spectral image by IHS transform and the panchromatic image are respectively contourlet transformed; Then, we select the low frequency information of multi-spectral image's Intensity component (*I*) as the low frequency information of fused image's Intensity component (*I*). After calculating and comparing with the matching degree of directional region between panchromatic image's and multi-spectral image's Intensity component (*I*) in high frequency coefficients, we further determine the fused image's Intensity component in high frequency coefficients. At last, the fused image can be obtained through inverse contourlet transform and inverse IHS transform. Simulation experiments show that our method can effectively improve spatial resolution and retain the color information of multi-spectral images. The entropy, joint entropy, average gradient and bias index, have all been achieved very well, so our method has a certain practicality.

REFERENCES

Asmare M H, Asirvadam V S and Iznita L. 2009. Multi-sensor image enhancement and fusion for vision clarity using contourlet transform. ICIME'09 International Conference on Information Management and Engineering. Los Alamitos: IEEE Computer Society Press

Chen M, Li D R, Qin Q Q and Jia Y H. 2006. Remote sensing image fusion based on contourlet transform. *Mini-Micro Systems*, **27**(11): 2052—2055

Chen T, Zhang J P and Zhang Y. 2005. Remote sensing image fusion based on ridgelet transform. IEEE International on Geoscience and Remote Sensing Symposium, **2**: 1150—1153

Choi M. 2006. A New Intensity hue saturation fusion approach to image fusion with a tradeoff parameter. *IEEE Transactions on Geoscience and Remote Sensing*, **44**(6): 1672—1682

Cunha A L , Zhou J P and Do M N. 2006. The nonsubsampled contourlet transform: Theory, design, and applications. *IEEE Trans. on Image Processing*, **16**(10):3089—3101

Di H W, Han Y D and Chen M S. 2006. An adaptive fusion method of multi-focus images. *Journal of Image and Graphics*, **11**(3): 353—356

Do M N and Vetterli M. 2005. The Contourlet transform: an efficient directional multi-resolution image representation. *IEEE Trans. Image Processing*, **14**(12):2091—2106

Feng P, Wei B, Pan Y J and Mi D L. 2008. Analysis of frequency aliasing of contourlet transform based on laplace pyramidal transform. *Acta Optica Sinica*, **28**(11): 2090—2096

Jiao L C and Tan S. 2003. Development and prospect of image multiscale geometric analysis. *Acta Electronica Sinica*, **31**(12A): 1975—1981

Li C J, Liu L Y, Wang J H, and Wang R C. 2004.Comparison of two methods of fusing remote sensing images with fidelity of spectral information. *Journal of Image and Graphics*, **9**(11): 1376—1387

Li Y, Xu X, Bai B D and Zhang Y N. 2008. Remote sensing image fusion based on fast discrete curvelet transform. Proceedings of the Seventh International Conference on Machine Learning and Cybernetics, Kunming China, **1**: 106—109

Lin X H, Zhang Y Z, and Yang Y J. 2009. Application of triangulation-based image registration method in the remote sensing image fusion. Proceedings of the 2009 International Conference on Environmental Science and Information Application Technology, Wuhan, China. **1**: 501—504

Liu K, Guo L and Chang W W. 2008. Regional feature self-adaptive image fusion algorithm based on contourlet transform. *Acta Optica Sinica*, **28**(4): 681—686

Liu Z, Hao C Y and Feng W. 2004. A remotely sensed image fusion method based on wavelet coefficient features. *Acta Geodaetica et Carorgraphica Sinica*, **33**(1): 53—57

Qu X B, Xie G F, Yan J W, Zhu Z Q and Chen B G. 2007. Image fusion algorithm based on neighbors and cousins information in nonsubsampled Contourlet transform domain. Proceedings of the 2007 International Conference on Wavelet Analysis and Pattern Recognition (ICWAPR '07),Beijing, China, **4**: 1797—1802

Tu T M, Huang P S, Hung C L and Chang C P. 2004. A fast intensity-hue-saturation fusion technique with spectral adjustment for IKONOS imagery. *IEEE Geoscience and Remote Sensing letters*, **1**(4): 309—312

Wu J, Liu Y, Liu J and Tian J W. 2006. Wavelet based remote sensing image fusion with color compensation rule and IHS transform. Proceedings of the 2006 IEEE International Conference on Mechatronics and Automation, 2079—2083

Zhang Q and Guo B L. 2008. Remote sensing image fusion based on the nonsubsampled contourlet transform. *Acta Optica Sinica*, **28**(1): 74—80

Zhang S Y, Wang P Q, Chen X Y and Zhang X. 2005. A new method for multi-source remote sensing image fusion. IEEE International on Geoscience and Remote Sensing Symposium, **6**: 3948—3951

Zheng Y A, Zhu C S. Song J S and Zhao X H. 2006. Fusion of multi-band SAR images based on contourlet transform. Proceedings of the 2006 IEEE International Conference on Information Acquisition, Sandong, China: 420—424

Contourlet 方向区域相关性的遥感图像融合

王相海[1,2], 魏婷婷[2], 周志光[3]

1. 辽宁师范大学 自然地理与空间信息科学辽宁省重点实验室, 辽宁 大连 116029;
2. 辽宁师范大学 计算机与信息技术学院, 辽宁 大连 116029;
3. 浙江大学 CAD&CG 国家重点实验室, 浙江 杭州 310027

摘 要: 对遥感图像经 Contourlet 变换后的高频子带系数分布的方向特征进行统计分析, 发现遥感图像经 Contourlet 变换后高频系数的分布具有较强的方向区域特征, 在此基础上, 提出一种基于 Contourlet 系数方向区域相关性的遥感图像融合算法, 该算法首先对多光谱图像经 IHS 变换后的亮度分量和全色图像分别进行 Contourlet 变换, 然后以多光谱图像亮度分量的低频信息作为融合图像亮度分量的低频信息, 通过计算并比较全色图像的高频系数和对应的多光谱图像亮度分量的高频系数的方向区域匹配度确定融合图像亮度分量的高频信息; 最后经过 Contourlet 逆变换和 IHS 逆变换获得融合图像。实验结果表明, 该算法在提高融合图像空间分辨率的同时能够更好地保留原始多光谱图像的光谱信息, 与传统遥感图像融合算法相比, 该算法具有较好的融合图像信息熵和清晰度, 具有一定的实用性。

关键词: 遥感图像融合, Contourlet 变换, 方向区域相关性, 融合算子

中图分类号: TP751.1 **文献标志码:** A

引用格式: 王相海, 魏婷婷, 周志光. 2010. Contourlet 方向区域相关性的遥感图像融合. 遥感学报, **14**(5): 905—916
Wang X H, Wei T T, Zhou Z G. 2010. Remote sensing image fusion method based on the contourlet coefficients' correlativity of directional region. *Journal of Remote Sensing*. **14**(5): 905—916

1 引 言

近年来, 遥感图像融合技术作为遥感图像处理技术的重要分支, 在资源调查、环境监测、区域分析及建设规划和全球性宏观研究等领域得到了广泛的应用和关注(李存军等, 2004; Lin 等, 2009; Li 等, 2008)。该技术通过处理低空间分辨率多光谱图像和高空间分辨率全色图像, 使得融合图像同时具有较高的光谱分辨率和较高的空间分辨率, 进而获得及时、可靠的遥感图像信息, 提高数据的使用效率(Zhang 等, 2005; Chen 等, 2005)。近年来比较流行的遥感图像融合方法有基于 IHS 变换的遥感图像融合方法、基于小波变换的遥感图像融合方法和基于 Contourlet 变换的遥感图像融合方法等 3 种, 其中, 第 1 种方法是利用全色图像替换掉多光谱图像经 IHS 变换后的亮度分量(Tu 等, 2004; Choi, 2006), 虽然提高了图像的空间分辨率, 但在一定程度上扭曲了融合图像的光谱特性, 产生了光谱失真现象; 第 2 种方法是在 IHS 变换的基础上, 利用小波变换的多尺度分析特性, 在一定程度上获得了较为丰富的高频细节信息(Wu 等, 2006; 刘哲等, 2004)。虽然小波变换在表示信号的点奇异性方面, 具有最优的逼近性能, 但是对于二维图像或者更高维的数据, 小波变换的稀疏表示能力比较有限。由于二维可分离小波的基函数, 其支撑区间为一个正方形, 且各向同性, 只能表示二维或高维信号在竖直、水平和对角线方向的直线奇异性。然而, 遥感图像中多数物体具有平滑边缘, 使得自然图像的奇异点往往不是独立分布的, 而是聚集成具有某些几何特征的奇异曲线。在这种情况下, 小波的各向同性的基函数不能有效地利用数据本身特有的几何特征捕获图像中沿着边缘方向的曲线奇异, 因此, 小波变换无法为图像提供最优的或者最稀疏的表示。在过去的几年中, 在小波变换的理论基础上发展起来的“多尺度

收稿日期: 2009-10-16; 修订日期: 2010-01-15

基金项目: 辽宁省自然基金项目(编号: 20072156)、辽宁“百千万人才工程”资助项目(编号: 2008921036)和南京邮电学院图像处理与图像通信江苏省重点实验室开放基金(编号: ZK207008)。

第一作者简介: 王相海(1965—), 男, 博士, 教授, 博士生导师, CCF 高级会员, 主要研究领域为多媒体信息处理, 计算机图形学。E-mail: xhwang@lnnu.edu.cn。

几何分析(multiscale geometric analysis, MGA)”(焦李成等, 2003)因其具有很好的各向异性特征, 成为处理二维图像及更高维数据的更优算法, 它很好地解决了小波变换不能有效地表示边缘、轮廓等高维奇异的问题。其中作为 MGA 的重要成员的 Contourlet 变换(Do & Vetterli, 2005)受到遥感图像融合领域的关注(Zheng 等, 2006; 陈蜜等, 2006; 张强 & 郭宝龙, 2008; 刘坤等, 2008), 在很大程度上改进了基于小波变换遥感图像融合算法中边缘和纹理信息融合不准的状况, 然而该研究领域才刚刚起步, 很多问题有待进一步研究, 遥感图像的融合质量还有待提高。

2 Contourlet 高频子带系数方向特性

Do 和 Vetterli(2005)在文献中提出了一种金字塔型方向滤波器组 PDFB(Pyramidal Directional Filter band), 称为轮廓波变换, 该变换首先对图像进行拉普拉斯金字塔(Laplacian Pyramid, LP)变换, 即对其进行多尺度分解以捕获二维图像中的奇异点, 经过拉普拉斯变换后的原始信号被分解为一个低频信息以及原始信号和预测信号的差值的带通信号; 然后对每一级金字塔分解的带通信号经由方向滤波器组(Directional Filter Bank, DFB)进行方向滤波, 使分布在同一方向的奇异点合成为一个系数, 其基的支撑区间具有随尺度而长宽比变化的“长条形”结构, 能有效地捕获图像中的线奇异性和面奇异性。所以, 这个结构使得 Contourlet 变换不仅具有较优的非线性逼近性能, 还具有多分辨率、局部定位、多方向性、近邻界采样和各向异性等性质, 与小波变换相比较, 能够更“稀疏”地表示图像(Asmare 等, 2009; Qu 等, 2007)。图 1 给出了 PDFB 对图像进行分解的过程示意图。图 2 给出了遥感图像经 Contourlet 变换分解实例。

传统的图像融合方法大多采用八邻域系数作为融合的判断依据(狄红卫等, 2006), 然而经过分析发现, 图像经 Contourlet 变换后, 各高频子带系数的分

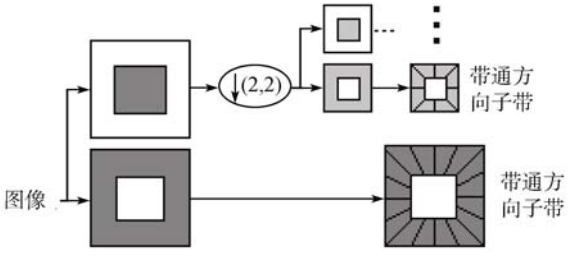

图 1 PDFB 对图像进行分解的过程示意图

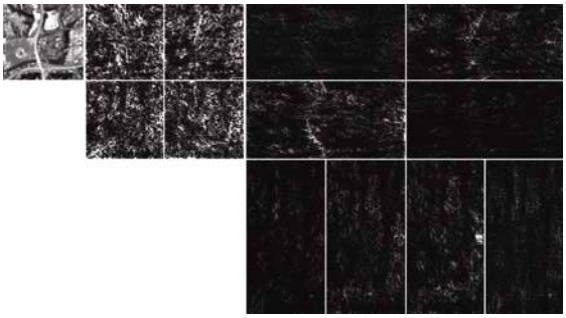

图 2 全色遥感图像 PAN 经 Contourlet 变换分解实例

布具有一定的方向区域特征。以图 3 所示的方向区域模板, 对大小为 256×256 的全色图像(Panchromatic, PAN)与多光谱图像(Multispectral, MS)的标准图像经 Contourlet 变换后的高频子带进行统计, 以方差作为区域相关性的衡量标准。若方向区域方差小于八邻域方差, 则表明方向区域相关性较强; 若方向区域方差大于八邻域方差, 则表明八邻域相关性较强。其中图 3(a)、3(b)的 4 个模板和 8 个模板分别对应如图 2 所示的图像经 Contourlet 变换后第 2 层 4 个不同方向子带和第 3 层 8 个不同方向子带。

统计所有高频系数的方向区域相关性, 结果如表 1, 其中子带 1—4 和子带 5—12 分别表示 Contourlet 变换后第 2 层高频的 4 个子带和第 3 层高频的 8 个子带方向区域相关性的统计数据, 即通过比较方向区域方差和八邻域方差的大小, 所获得的满足方向区域相关性的系数占该子带系数总和的比例。从表 1 看出, 高频子带系数中满足方向区域相关性的系数所占比例均超过 50%, 这表明变换后的高频子带各系数方向区域相关性明显比八邻域相关性强。

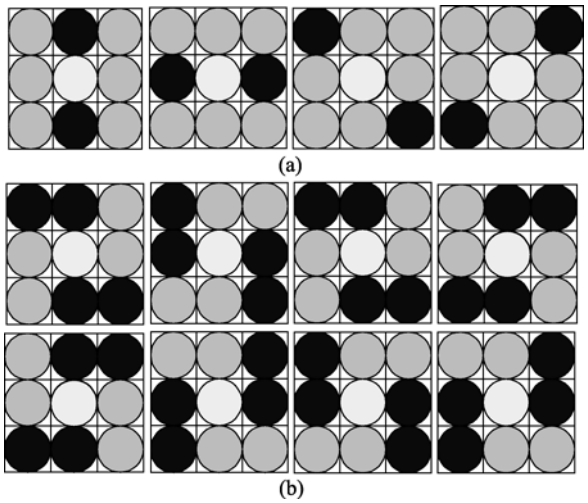

图 3 遥感图像 Contourlet 高频子带采用的方向区域模板
(a) 对应 Contourlet 变换第二层四个子带的模板;
(b) 对应 Contourlet 变换第三层八个子带的模板

表 1 PAN 图像与 MS 图像方向区域相关性统计数据

子带	全色 PAN/%	多光谱 MS *R*/%	多光谱 MS *G*/%	多光谱 MS *B*/%
1	82.23	91.02	89.85	90.45
2	62.59	59.60	60.04	59.68
3	75.91	72.71	72.87	73.83
4	81.63	90.63	90.45	90.11
5	59.86	58.15	58.61	58.60
6	58.46	60.59	60.33	60.59
7	55.54	54.26	53.60	54.34
8	55.93	55.94	55.34	55.90
9	57.57	58.35	58.36	58.53
10	56.89	60.23	60.91	61.19
11	58.56	59.87	60.36	60.20
12	56.93	56.69	57.23	57.28

注: R: Red; G: Green; B: Blue

3 基于 Contourlet 系数方向区域相关性的遥感图像融合算法

3.1 算法的基本过程

由第 2 节的分析和统计结果可知遥感图像 Contourlet 变换的高频子带系数具有一定的方向区域特征，这种方向特性使得在不同的高频子带中，当前融合系数与其周围的 8 个相邻系数的“密切”程度不尽相同，这样如果采用与融合系数关系比较紧密的系数确定融合规则势必会提高最后的融合图像效果。

与传统的 Contourlet 系数替换的融合算法不同，本文算法根据遥感图像 Contourlet 变换高频子带的方向区域特性，利用所给出的方向区域模板捕捉各子带的方向系数，通过比较待融合系数的方向区域匹配度确定融合算子，从而更准确的确定融合图像 *I* 分量的高频系数。算法总体流程如图 4。

算法如下:

步骤 1 对多光谱图像进行 IHS 变换;

步骤 2 对 IHS 变换后的多光谱图像 *I* 分量和全色图像分别进行 Contourlet 变换;

步骤 3 以多光谱图像亮度分量的低频信息作为融合图像 *I* 分量的低频信息;

步骤 4 计算并比较全色图像的高频系数和对应的多光谱图像 *I* 分量的高频系数的方向区域匹配度，进而确定融合图像 *I* 分量的高频系数;

步骤 5 通过 Contourlet 逆变换获得融合图像的 IHS 变换结果;

步骤 6 通过 IHS 逆变换获得融合图像。

3.2 融合算子的选取

由于多光谱图像具有较强的光谱特性，背景信息比较显著，在对多光谱图像 IHS 变换后的 *I* 分量和全色图像分别经 Contourlet 变换后，在低频系数的融合过程中，我们以多光谱图像亮度分量的低频信息作为融合图像亮度分量的低频信息，从而保证了融合图像的多光谱特征；在对高频系数融合的过程中，利用本文第 2 节获得的方向区域模型，提出 Contourlet 系数方向区域相关性融合算子，具体步骤如下:

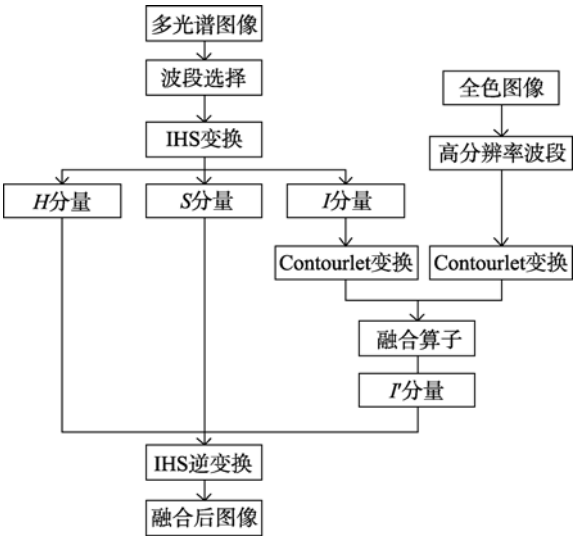

图 4 本文算法基本过程图

步骤 1 通过下面公式(1)计算相应位置高频系数的方向区域能量，其中，α表示方向模板，对不同的子带选取不同的方向模板(参见图 3); $f_k(i,j)$和 $E_k(i,j)$ 分别表示第 $k(k=1,2)$幅图像方向区域内的待融合系数和对应位置系数所在方向模板的区域能量。

$$E_k(i,j)=\sum_{f_k(i,j)\in\alpha}(f_k(i,j))^2 \tag{1}$$

步骤 2 通过公式(2)计算相应位置高频系数的方向区域匹配度。其中, $M(x,y)$表示两幅图像对应位置高频系数的方向区域匹配度。

$$M(i,j)=\frac{2\sum_{f_k(i,j)\in\alpha}(f_1(i,j)\cdot f_2(i,j))}{E_1(i,j)+E_2(i,j)} \tag{2}$$

步骤 3 将步骤 2 中求出的方向区域匹配度与阈值β进行比较(β可通过试验统计获得，本文后面的试验中选取其为 0.9)，进而确定融合图像的高频系数，具体操作如下:

若 $M(x,y)<\beta$

$$f(x,y)=\begin{cases}f_1(x,y) & \text{if} \quad E_1>E_2\\ f_2(x,y) & \text{others}\end{cases}$$

若 $M(x,y)\geqslant\beta$，则

$$f(x,y)=\begin{cases}w_{\max}f_1(x,y)+w_{\min}f_2(x,y) & \text{if} \quad E_1>E_2\\ w_{\min}f_1(x,y)+w_{\max}f_2(x,y) & \text{others}\end{cases}$$

其中 $w_{\min}=\dfrac{1-M(x,y)}{2(1-\beta)}$、$w_{\max}=1-w_{\min}$ 分别为待融合系数的加权系数，$f(x,y)$为最终的融合系数；

步骤 4　按照上述步骤，遍历不同方向高频子带的所有系数点，最终获得融合图像 I 分量的高频子带系数。

4　试验与分析

为了验证本文算法的有效性，对如下 3 组标准的遥感图像进行了仿真试验：第 1 组分辨率为 80m 的 MS 多光谱图像与分辨率为 32m 的 PAN 高分辨率图像；第 2 组图像来自 ERDAS 例子库的 TMS 图像与 SPOTS 图像；第 3 组来自美国 Landsat5 拍摄的多光谱 TM 图像与法国 SPOT 卫星拍摄的高分辨率图像。本文算法与传统的基于 IHS 变换的遥感图像融合方法、基于小波变换的遥感图像融合方法以及基于 Contourlet 变换的遥感图像融合方法进行了比较，图 5—图 7 分别为对 3 组图像的相应融合结果。

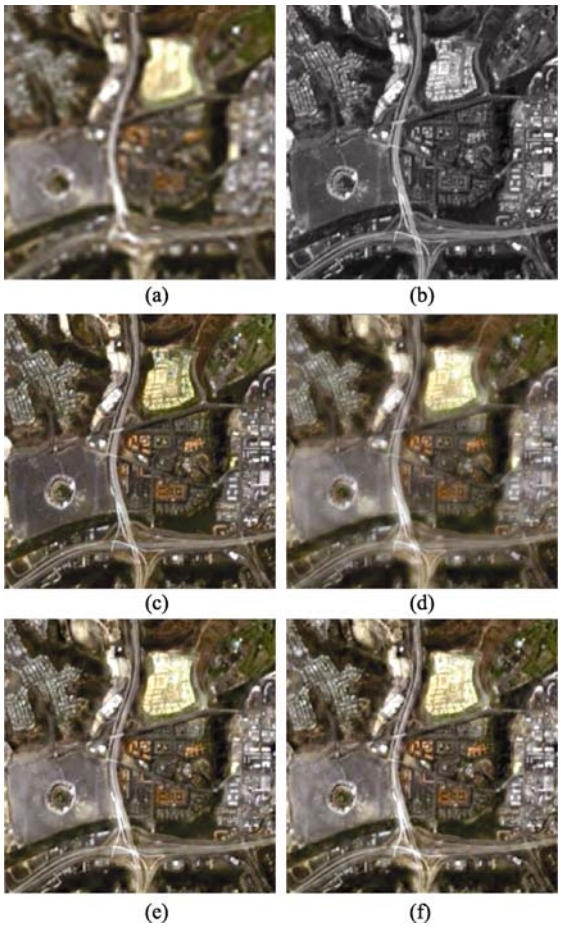

图 5　MS 与 PAN 图像的融合图像比较

(a) 多光谱图像 MS; (b) 全色图像 PAN; (c) IHS 变换算法; (d) 小波+IHS 变换算法; (e) Contourlet 高频替换算法; (f) 本文算法

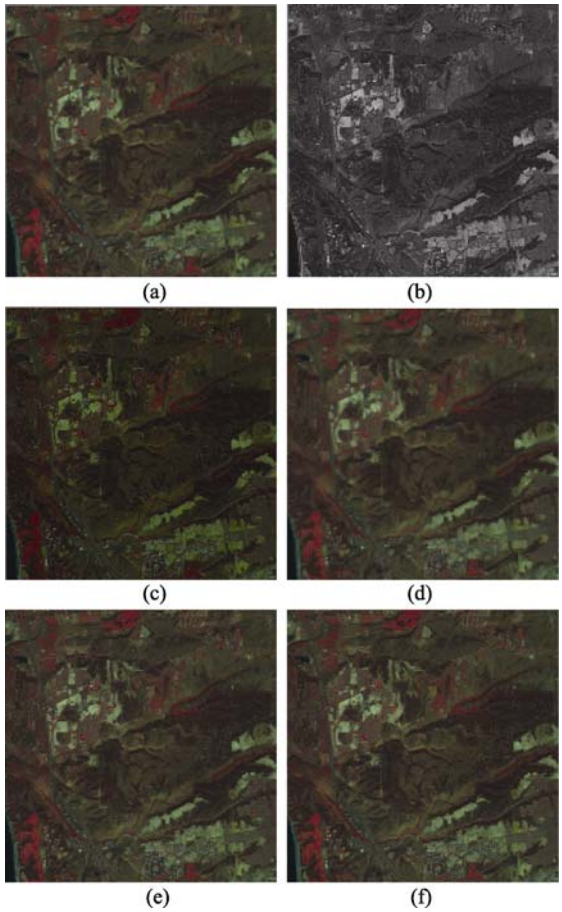

图 6　TM 与 SPOT 图像的融合图像比较

(a) 多光谱图像 TM; (b) 全色图像 SPOT; (c) IHS 变换算法; (d) 小波+IHS 变换算法; (e) Contourlet 高频替换算法; (f) 本文算法

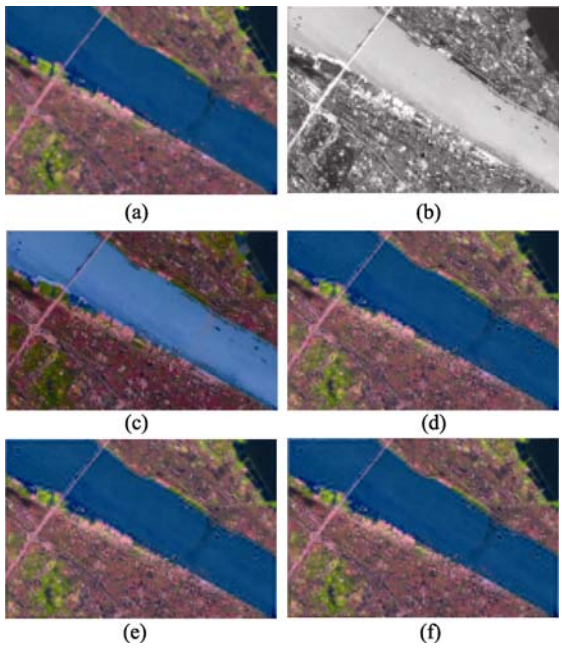

图 7　TM 与 SPOT 图像的融合图像比较

(a) 多光谱图像 TM; (b) 全色图像 SPOT; (c) IHS 变换算法; (d)小波+IHS 变换算法; (e) Contourlet 高频替换算法; (f) 本文算法

由图 5—图 7 试验结果看出，与传统方法相比，本文算法所得到的融合结果纹理和色彩更加清晰，光谱特性也得到了很好的保留。

此外，为了定量的比较各融合算法的性能，表 2 给出了各融合算法融合图像的信息熵、联合熵、平均梯度和偏差指数等客观评价指标的统计结果。由表 2 看出，采用本文算法所获得的融合图像，在信息熵、联合熵、平均梯度和偏差指数等方面均取得了较好的结果，具体: (1)本文算法在处理 MS 图像与 PAN 图像时，能够在加强融合图像空间分辨率的同时，更好地保留图像的光谱分辨率；(2)本文算法在处理 TM 图像与 SPOT 图像时，信息熵、联合熵、平均梯度是所有算法中最大的，偏差指数是四者中最小的，这表明本文算法较好地保留了图像的空间分辨率和光谱分辨率；(3)本文算法在处理 TM 图像与 SPOT 图像时，信息熵、联合熵的值不及 IHS 变换，而平均梯度是所有算法中最显著的，且偏差指数是最小的，这说明 IHS 变换以牺牲光谱信息换取了空间信息，虽然图像略显清晰，但光谱失真较为严重，而本文算法在提高空间细节信息的同时较好地保留了原始图像的光谱信息，光谱失真较小，算法具有一定的实用性。

虽然 Contourlet 变换相对于小波变换各向异性特征明显，在边缘、轮廓的提取方面有较大优势，然而，由于 Contourlet 的 LP 变换中两个低通滤波器不满足 Nyquist 抽样定律，致使阻带截至频率大于π/2，导致 Contourlet 变换的频谱混叠(冯鹏等, 2008)，产生伪吉布斯现象，从而对图像的融合结果产生一定的影响。近年来，出现了一些抗混叠的 Contourlet 变换，比较典型的是基于非下采样的 Contourlet 变换(Cunha 等, 2006)，该变换具有平移不变特性，克服了频率的混叠效应。然而通过大量试验发现，经过该变换后的子带系数，其方向特性较传统的 Contourlet 变换弱化了，并且基于该变换图像融合的空间和时间复杂度均较高，这在一定程度上影响了图像融合的实时处理。本文在权衡了融合效率和融合效果，利用 Contourlet 变换各高频子带内部系数之间存在较强的方向区域相关特性，确定了相应的融合算子，该算子突出和强调了各子带系数的区域方向特性，从试验结果看出，与传统的 Contourlet 替换算法相比，在一定程度上改善了频率混叠效应所带来的影响。

表 2 算法的信息熵、联合熵、平均梯度和偏差指数统计结果

评价标准 \ 算法			IHS 变换	小波变换+HIS 变换	Contourlet 替换	本文算法
信息熵	第一组实验	*R*	6.7339	7.5222	7.5201	7.5417
		G	6.6053	7.4974	7.4938	7.5159
		B	6.2987	7.4875	7.4868	7.5057
	第二组实验	*R*	5.9393	6.2173	6.2178	6.2197
		G	6.2169	6.3742	6.3741	6.3789
		B	5.6608	5.7921	5.7927	5.7909
	第三组实验	*R*	6.9112	7.0800	7.1189	7.1225
		G	6.6743	6.3017	6.3372	6.3381
		B	7.0773	6.5630	6.6185	6.6074
联合熵	第一组实验		19.6379	22.5071	22.5007	22.5646
	第二组实验		17.8170	18.3837	18.3846	18.3895
	第三组实验		20.6628	19.9447	20.0745	20.0680
平均梯度	第一组实验	*R*	4.0386	4.4337	4.4320	4.7659
		G	3.9484	4.3637	4.3552	4.6900
		B	3.8127	4.3660	4.3600	4.6814
	第二组实验	*R*	3.3845	3.4358	3.4325	3.4463
		G	3.3906	3.4407	3.4372	3.4563
		B	3.3160	3.3516	3.3477	3.3530
	第三组实验	*R*	3.7002	3.7966	3.7847	3.8747
		G	3.3228	3.4175	3.4064	3.4751
		B	3.4723	3.4672	3.4561	3.4846
偏差指数	第一组实验		0.0285	0.0929	0.1098	0.0651
	第二组实验		0.0051	0.0176	0.0179	0.0164
	第三组实验		0.3847	0.0146	0.0219	0.0129

5 结 论

本文首先对遥感图像经 Contourlet 变换后高频子带系数的方向区域相关性进行了分析，发现图像经 Contourlet 变换后，各个高频子带系数的分布具有一定的方向区域特征，统计结果验证了该结论，同时给出了用于统计各高频子带方向区域特性的方向区域模板。在此基础上，提出了一种新的基于 Contourlet 系数方向区域相关性的遥感图像融合算法，算法首先对多光谱图像经 IHS 变换后的亮度分量和全色图像分别进行 Contourlet 变换，然后以多光谱图像亮度分量的低频信息作为融合图像亮度分量的低频信息，在高频信息的选择过程中，通过计算并比较全色图像的高频系数和对应的多光谱图像亮度分量的高频系数的方向区域匹配度，确定融合图像亮度分量的高频系数，最后经过 Contourlet 逆变换和 IHS 逆变换即可获得融合图像。仿真试验表明，本文算法能够有效的提高融合图像的空间分辨率和保留多光谱图像的光谱信息，算法融合图像的信息熵、联合熵、平均梯度和偏差指数等客观评价指标均取得了很好的效果，算法具有一定的实用性。

REFERENCES

Asmare M H, Asirvadam V S and Iznita L. 2009. Multi-sensor image enhancement and fusion for vision clarity using contourlet transform. ICIME’09 International Conference on Information Management and Engineering. Los Alamitos: IEEE Computer Society Press

Chen M, Li D R, Qin Q Q and Jia Y H. 2006. Remote sensing image fusion based on contourlet transform. *Mini-Micro Systems*, **27**(11): 2052—2055

Chen T, Zhang J P and Zhang Y. 2005. Remote sensing image fusion based on ridgelet transform. IEEE International on Geoscience and Remote Sensing Symposium, **2**: 1150—1153

Choi M. 2006. A New Intensity hue saturation fusion approach to image fusion with a tradeoff parameter. *IEEE Transactions on Geoscience and Remote Sensing*, **44**(6): 1672—1682

Cunha A L , Zhou J P and Do M N. 2006. The nonsubsampled contourlet transform: Theory, design, and applications. *IEEE Trans. on Image Processing*, **16**(10):3089—3101

Di H W, Han Y D and Chen M S. 2006. An adaptive fusion method of multi-focus images. *Journal of Image and Graphics*, **11**(3): 353—356

Do M N and Vetterli M. 2005. The Contourlet transform: an efficient directional multi-resolution image representation. *IEEE Trans. Image Processing*, **14**(12): 2091—2106

Feng P, Wei B, Pan Y J and Mi D L. 2008. Analysis of frequency aliasing of contourlet transform based on laplace pyramidal transform. *Acta Optica Sinica*, **28**(11): 2090—2096

Jiao L C and Tan S. 2003. Development and prospect of image multiscale geometric analysis. *Acta Electronica Sinica*, **31**(12A): 1975—1981

Li C J, Liu L Y, Wang J H, and Wang R C. 2004.Comparison of two methods of fusing remote sensing images with fidelity of spectral information. *Journal of Image and Graphics*, **9**(11): 1376—1387

Li Y, Xu X, Bai B D and Zhang Y N. 2008. Remote sensing image fusion based on fast discrete curvelet transform. Proceedings of the Seventh International Conference on Machine Learning and Cybernetics, Kunming China, **1**: 106—109

Lin X H, Zhang Y Z, and Yang Y J. 2009. Application of triangulation-based image registration method in the remote sensing image fusion. Proceedings of the 2009 International Conference on Environmental Science and Information Application Technology, Wuhan, China. **1**: 501—504

Liu K, Guo L and Chang W W. 2008. Regional feature self-adaptive image fusion algorithm based on contourlet transform. *Acta Optica Sinica*, **28**(4): 681—686

Liu Z, Hao C Y and Feng W. 2004. A remotely sensed image fusion method based on wavelet coefficient features. *Acta Geodaetica et Carorgraphica Sinica*, **33**(1): 53—57

Qu X B, Xie G F, Yan J W, Zhu Z Q and Chen B G. 2007. Image fusion algorithm based on neighbors and cousins information in nonsubsampled Contourlet transform domain. Proceedings of the 2007 International Conference on Wavelet Analysis and Pattern Recognition (ICWAPR '07),Beijing, China, **4**: 1797—1802

Tu T M, Huang P S, Hung C L and Chang C P. 2004. A fast intensity-hue-saturation fusion technique with spectral adjustment for IKONOS imagery. *IEEE Geoscience and Remote Sensing letters*, **1**(4): 309—312

Wu J, Liu Y, Liu J and Tian J W. 2006. Wavelet based remote sensing image fusion with color compensation rule and IHS transform. Proceedings of the 2006 IEEE International Conference on Mechatronics and Automation, 2079—2083

Zhang Q and Guo B L. 2008. Remote sensing image fusion based on the nonsubsampled contourlet transform. *Acta Optica Sinica*, **28**(1): 74—80

Zhang S Y, Wang P Q, Chen X Y and Zhang X. 2005. A new method for multi-source remote sensing image fusion. IEEE International on Geoscience and Remote Sensing Symposium, **6**: 3948—3951

Zheng Y A, Zhu C S. Song J S and Zhao X H. 2006. Fusion of multi-band SAR images based on contourlet transform. Proceedings of the 2006 IEEE International Conference on Information Acquisition,Sandong, China: 420—424

附中文参考文献

陈蜜，李德仁，秦前清，贾永红. 2006. 基于 Contourlet 变换的遥感影像融合算法. 小型微型计算机系统, **27**(11): 2052— 2055

狄红卫，韩耀东，陈木生. 2006. 一种自适应的多聚焦图像融合方法. 中国图象图形学报, **11**(3): 353—356

冯鹏，魏彪，潘英俊，米德伶. 2008. 基于拉普拉斯塔型变换的 Contourlet 变换频谱混叠特性分析. 光学学报，**28**(11): 2090—2096

焦李成，谭山. 2003. 图像的多尺度几何分析：回顾和展望. 电子学报, **31**(12A): 1975-1981

李存军，刘良云，王纪华，王人潮. 2004. 两种高保真遥感融合影像方法比较. 中国图象图形学报, **9**(11): 1376—1387

刘坤，郭雷，常威威. 2008. 基于 Contourlet 变换的区域特征自适应图像融合算法. 光学学报, **28**(4): 681—686

刘哲，郝重阳，冯伟. 2004. 一种基于小波系数特征的遥感图像融合算法. 测绘学报, **33**(1): 53—57

张强，郭宝龙. 2008. 基于非采样 Contourlet 变换的遥感图像融合算法. 光学学报, **28**(1): 74—80